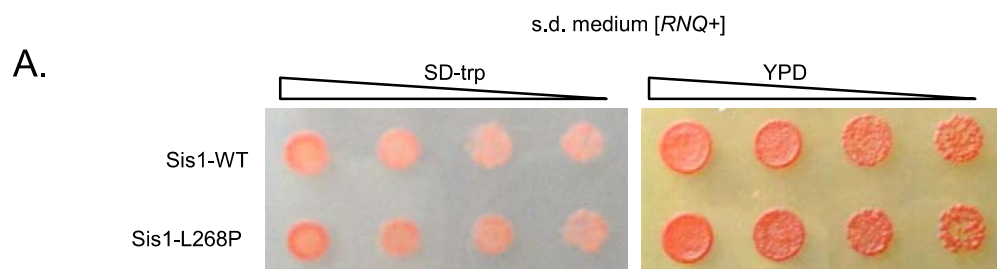
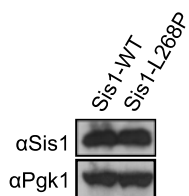


Figure S1

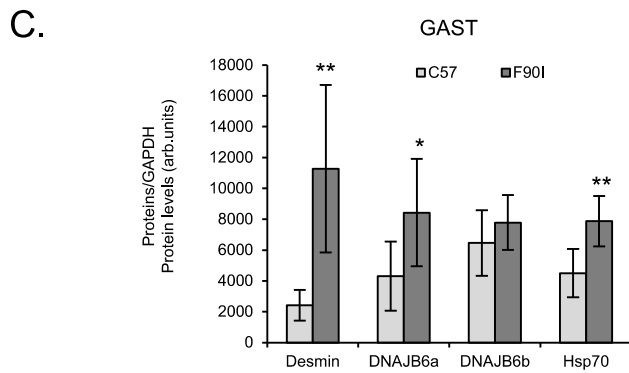
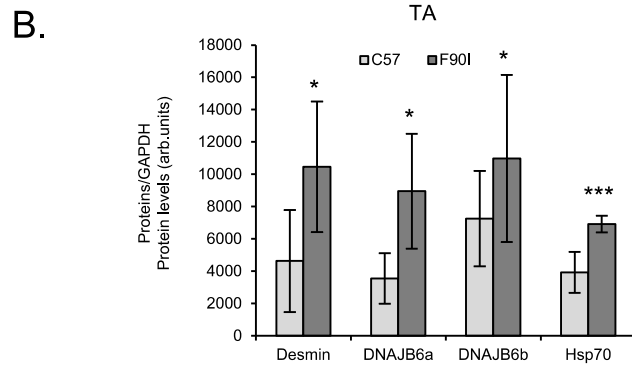
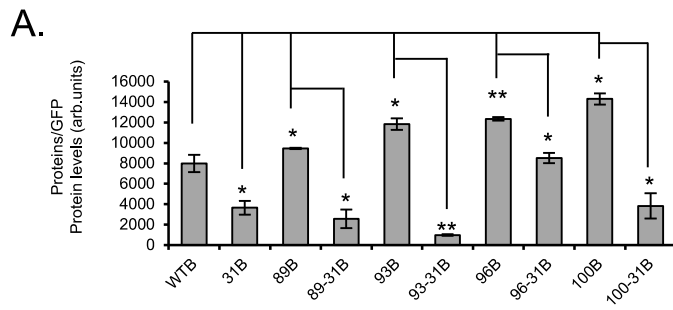


B.



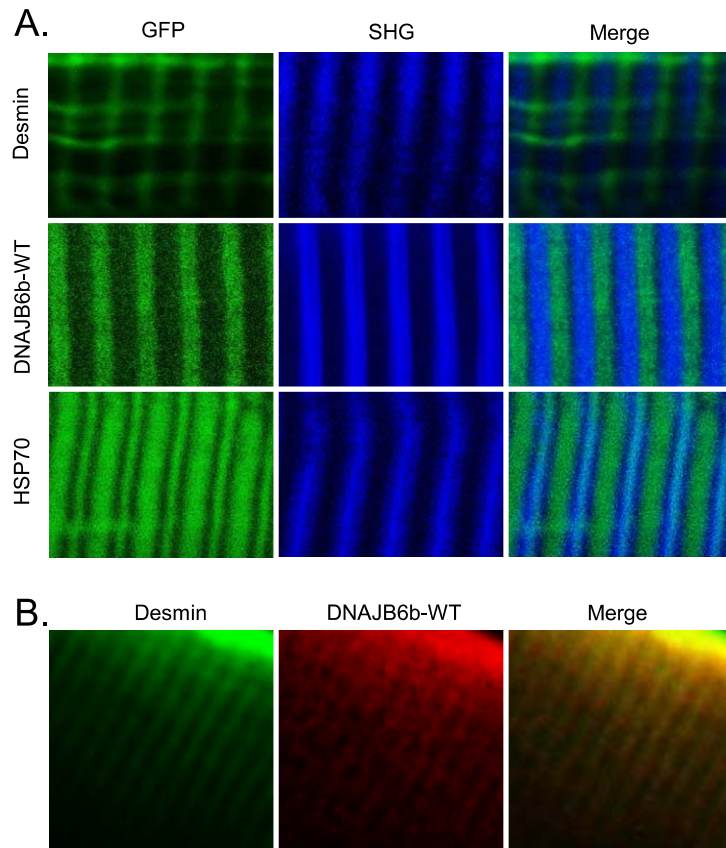
**A)** Yeast cells propagating m.d. high [RNQ+] were transformed with plasmids over-expressing Sis1-WT, Sis1-L268P. Cultures were normalized and serially diluted five-fold and were spotted on medium (SD-trp) to select for the plasmid or medium (YPD) that provides no selection. Notice that there is no difference in viability of the second Sis1 mutant construct (L268P) vs Sis1-WT. **B)** Western blot analysis were performed to show the expression of Sis1 in the indicated constructs. Notice that there was no significant difference in the expression of Sis1-L268P vs Sis1-WT. Pgk1 was used as a loading control. Images for both (A) and (B) are representative of three independent experiments.

Figure S2



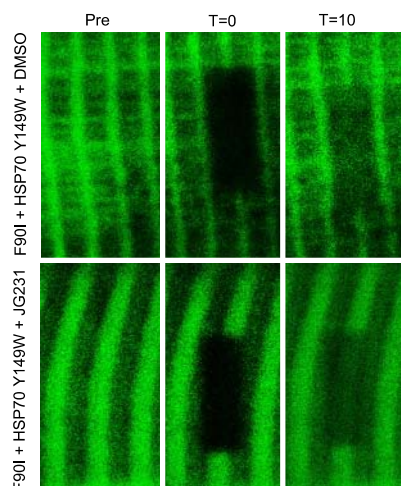
**A)** Densitometric quantitation of 3 independent experiments from the results represented in Figure 3A. **B-C)** Densitometric quantitation of 3 independent experiments from the results represented in Figure 4G.

Figure S3

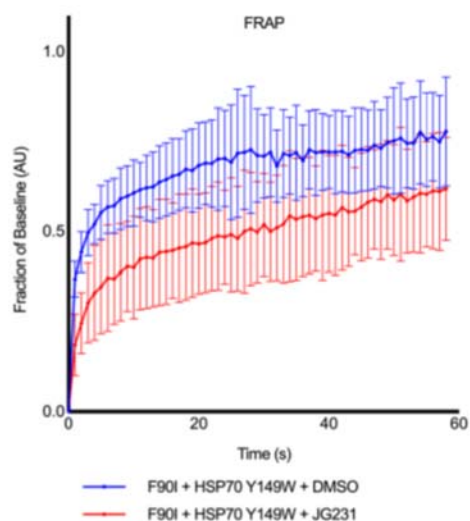


**A)** Desmin-GFP, GFP-DNAJB6b-WT and HSP70-GFP were electroporated in mouse FDB muscle and live mouse footpad was imaged via two-photon microscopy. Second harmonic generation was concurrently imaged to visualize the A-band for a reference point. **B)** Co-electroporation of Desmin-GFP and mCherry-DNAJB6b-WT mouse FDB.

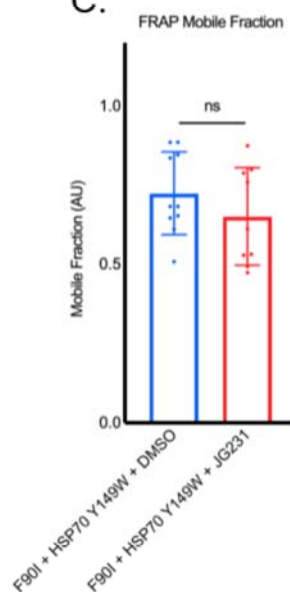
A.



B.

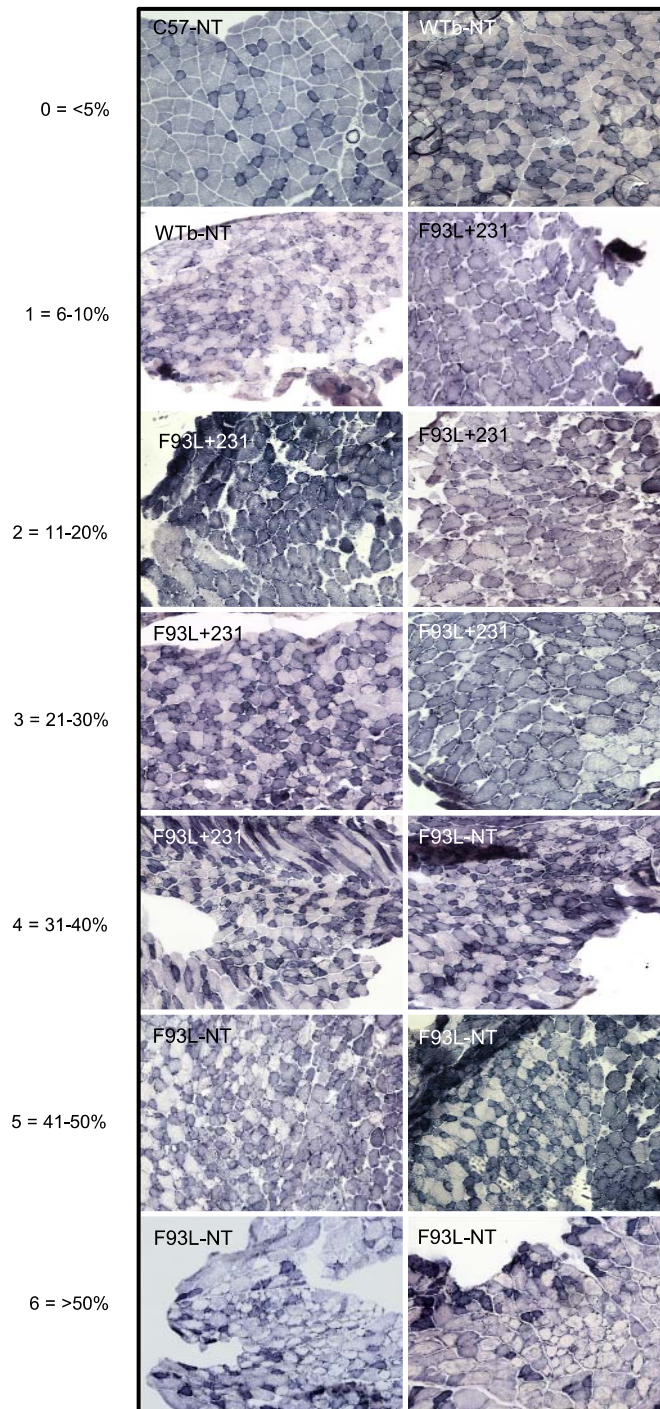


C.



**A-C)** Fluorescence recovery after photobleaching was performed with two-photon microscopy on mouse foot pad following electroporation into the FDB with constructs expressing HSP70-Y149W-GFP into DNAJB6-F90I heterozygous mice. In some cases, mice were giving i.p. injections of JG231. **A)** Representative images show baseline prior to bleaching (pre), immediately post-bleach (t=0s), and following (10s) of recovery (t=10s). **B)** Graph of the normalized RFI vs time in seconds for the studies in (A). **C)** Graph of the percentage of maximum fluorescence recovery corresponding to the mobile vs immobile fraction from (A).

Figure S5



Examples of NADH myofibrillar disorganization scoring key. The score given was based on the estimated % of muscle fibers with abnormal staining, as denoted to the left of the example pictures. NADH staining was considered abnormal based on the presence of an irregular, reduced, or absent staining pattern.

Figure S6

Hspb8 rev-qPCR mouse	TTG GTG AAG TTC TTG GAG ACA AT
Hsph1 fwd-qPCR mouse	AAC CCC AGA TGC TGA CAA AG
Hsph1 rev-qPCR mouse	CCA CCT TTA TTT TAG GTT TCT TGG
GAPDH-Left	ATG GTG AAG GTC GGT GTG A
GAPDH-Right	AAT CTC CAC TTT GCC ACT GC
Bag 1-fwd qPCR mouse	GCT AAC CAC CTG CAA GAA TTG
Bag 1-rev qPCR mouse	TTG CAA TTC CTT AGC CAG AAA
Bag 3-fwd qPCR mouse	CCA ACT GCT CAT GGA CCT G
Bag 3-rev qPCR mouse	GCC GAG GAG GAA GAG GAT
Cryab-fwd qPCR mouse	ACG GCA AGC ACG AAG AAC
Cryab-rev qPCR mouse	TCC GGT ACT TCC TGT GGA AC
Dnaja1-fwd qPCR mouse	TGG CTC TGC AAA AGA ATG TG
Dnaja1-rev qPCR mouse	TGA ATC CTT ATC TGC ATA CCT GTC
Dnaja2-fwd qPCR mouse	TGG ATC AAC CCA GAC AAA CTT
Dnaja2-rev qPCR mouse	CTC CAA TAA CAT TAG GAA CTT CTG G
Dnajb2-fwd qPCR mouse	AGC TCG CCA TGG CTT ACA
Dnajb2-rev qPCR mouse	TGG AAC TGC AGC AAC TCT GT
Dnajb9-fwd qPCR mouse	CAC AAA GAT GCC TTT TCT ACC G
Dnajb9-rev qPCR mouse	TTA AAC TTT TCA GCT TAA TGA CGT G
Dnajb6 rev-qPCR human	TTC ATA TGC CTC CGC TAC TTG
Dnajb6 fwd-qPCR human	ATG AAG TTC TAG GCG TGC AG
p62(Sqstm1)-Left	GAA GCT GCC CTA TAC CCA CA
p62(Sqstm1)-Right	TGG GAG AGG GAC TCA ATC AG
FHL1 mouse-Left	AAGTGTGCTGGATGCAAGAA
FHL1 mouse-Right	GGGTGGCTCACTCTTGACAC
DES mouse qPCR fwd	TGCAGCCACTCTAGCTCGTA
DES mouse qPCR rev	TGAAGCTCACGGATCTCCTC
SYMN mouse qPCR fwd	AGCTCCTATCCCAGACAAGGT
SYMN mouse qPCR rev	CGACACTTTGGTGTGCTCAG
TDP43 mouse qPCR fwd	AGCATTAAACCCAGCGATGAT
TDP43 mouse qPCR rev	ATGCCCCATCATACCCCAAC
DNAJC12 mouse fwd	GAGGACTACTACGCCTTGCTG
DNAJC12 mouse rev	AATTCTGCCAAGATTTGCTCA
DNAJC15 mouse fwd	CCGACATCGACCACACAG
DNAJC15 mouse rev	AACAGCTGCAACACCTAGTCC
Dnajc6 fwd-qPCR mouse	GGC TCT CCG GGT GTA AAG A
Dnajc6 rev-qPCR mouse	CAT AGC TGG GCT CCA TGT CT
Hsf 2 fwd-qPCR mouse	ACC CAC ACC AAC GAG TTC AT
Hsf 2 rev-qPCR mouse	TGC TCA TCC AAG ACC AGA AA
Hsp90aa 1 fwd-qPCR mouse	GTC TCG TGC GTG TTC ATT CA
Hsp90aa 1 rev-qPCR mouse	CAT TAA CTG GGC AAT TTC TGC
Hsp90b 1 fwd-qPCR mouse	AGG GTC CTG TGG GTG TTG
Hsp90b 1 rev-qPCR mouse	CAT CAT CAG CTC TGA CGA ACC
Hspa1a fwd-qPCR mouse	GGC CAG GGC TGG ATT ACT
Hspa1a rev-qPCR mouse	GCA ACC ACC ATG CAA GAT TA
Hspb8 fwd-qPCR mouse	CCA AGG ATG GAT ACG TGG AA
Hspb8 rev-qPCR mouse	TTG GTG AAG TTC TTG GAG ACA AT
Hspb7 fwd-qPCR mouse	TGC CTA CGA GTT TAC AGT GGA C
Hspb7 rev-qPCR mouse	TTC ATG ACT GTG CCA TCA GC

qPCR primers